International Journal for Multidisciplinary Research (IJFMR)
E-ISSN: 2582-2160 ● Website: www.ijfmr.com ● Email: editor@ijfmr.com

Application of BSA Optimised I-TD Controller in A Two Area Automatic Generation Control System

Nitesh Kumar[1], Sanjeev Kumar Bhagat[2], Pooja Jha[3]

[1]PG Scholar, Electrical Engineering, Sandip University
[2]Assistant Professor, Electrical Engineering, Sandip University
[3]Assistant Professor (H.O.D), Electrical Engineering, Sandip University

Abstract
This study presents the application of a Bird Swarm Algorithm optimised Integral minus Tilt Derivative controller for a two area automatic generation control system. The objective is to enhance frequency stability and tie line power regulation under sudden load disturbances and variable operating conditions. A detailed mathematical model of the interconnected system is developed and the BSA technique is employed to tune the controller parameters effectively. The proposed controller is compared with conventional PID, TID and I TD structures using settling time and integral time absolute error as performance indices. Simulation results confirm that the optimised controller provides faster damping of oscillations, reduced frequency deviation and improved robustness against load variations. The method demonstrates reliable dynamic performance and better adaptability to different loading scenarios in comparison with existing approaches.

Keywords: Automatic Generation Control, Bird Swarm Algorithm, I-TD Controller, Frequency Regulation, Two Area Power System, ITAE.

1. Introduction

The ongoing growth of the modern power system (PS) has resulted in a considerable increase in its inherent complexity. Keeping the normal system frequency and balancing the production and demand sides of megawatt electricity are both made more difficult by this expansion. These problems are effectively handled by Automatic Generation Control (AGC). The fundamental objective of this mechanism is to develop a reliable control system that can distribute power between the generator and the load in a way that keeps the frequency profile constant throughout the whole linked system [1,2]. To keep the system frequency and tie-line powers at their nominal levels, AGC is also crucial in large-scale, linked power systems across several areas. A drop in the frequency of producing units is common when the produced active power falls short of the power demand, whether as a result of unexpected disruptions or any other cause [1,2]. Unwanted deviation from the nominal value of the
system frequency occurs as a result of this. Using the AGC idea, the frequency variation can be promptly dampened and the tie-line power can be maintained at its planned value. But the speed governor can't get the consistent frequency on his own. Therefore, a control mechanism is necessary to

neutralize the impact of unexpected variations in load and maintain the frequency at its nominal value [3].

Despite the dearth of data, experts from all over the globe have spent decades attempting to decipher the AGC issue by using a variety of control schemes and optimization methodologies. For an AGC issue, studies have utilized and compared the following concepts: "optimum control theory [4], integral [5], proportional-integral, proportional-integral-derivative, fractional order PID, and proportional-integral-double derivative [3]." Tuning PI controllers for multi-area power systems is suggested by Daneshfar and Bervani [6] using the multi-objective optimization problem (MOP) method and the Genetic Algorithm (GA) technology. In a two-area linked thermal power system, Gozde et al. [7] investigated the AGC's dynamic performance using the Artificial Bee Colony (ABC) optimization method. After comparing the BFOA method to GA and Ziegler Nichols (ZN), Ali and Abd Elazim [8] optimized the gains of a PID controller for an LFC issue.

Over the last sixty years, several studies have documented various approaches to solving the AGC issue in distributed power systems [9, 10]. The design of AGC controllers has made use of many control methods to improve dynamic performance. The conventional proportional-integral (PID) controller and the proportional-integral-derivative (PID) controller are the two most common kinds of AGC controllers. Then, taking into account generation rate limits, [11] addressed AGC of a multi-area hydro-thermal system. The electric governor and integral controller settings were optimized using the ISE criteria. Prior research focused on determining an appropriate value for the governor speed control parameter and investigating how the strength of the tie lines affected the dynamic response. However, power system engineers were inspired to create new AGC tactics by the advent of fast digital computers, advancements in optimal control theory, and the vast capabilities of these computers to handle massive amounts of data with various types of interconnections.

Numerous research publications [9] on AGC controller designs have laid the groundwork for more sophisticated controllers based on intelligent techniques (IT) for AGC applications in power systems, building on the foundation of classical controllers. A five-area linked power system with reheat turbines was the subject of Akanksha, et.al.'s [12] Automatic Generation Control (AGC]. In this case, the ANN controller coordinates the inputs to the power supply across all areas. In contrast to the traditional integral controller, the suggested controller uses the load perturbation as an input control signal to enhance controller performance. The controller is shown to be practically relevant to power systems in the real world, and a backpropagation algorithm is developed. The results show that when comparing the two types of controllers, ANN performs better in terms of peak overshoot and settling time compared to integral controller. "Whal [13], Grey Wolf [14], sine cosine [15], crow [16], particle swarm [17], hybrid crow [18], genetic [19], ant lion [20], Cuckoo Search [21], firefly [22], crow search [23], moth fly [24], tunicate swarm [25], reinforcement learning [26], and hawk optimization [27]" are some of the optimization algorithms that have recently emerged as effective in AGC research. Among them, BSA stands out for its ability to enhance controller performance in different AGC setups.

Motivated by the coordinated foraging actions of flocks of birds, Meng [28] presented the BSA algorithm. Fast convergence, excellent precision, and fewer iterations are the hallmarks of this approach to global optimization [29, 30]. However, a two-area AGC system has not yet investigated its feasibility for optimizing an Integral minus Tilt Derivative (I-TD) controller. In order to study the dynamics of the system, many secondary controllers, including TID and PID, are applied separately. The BSA is used, which is a new metaheuristic optimization method.

A. AGC Algorithm for Two-Area Power System

The popular AGC algorithm uses a linear equation called the area control error (ACE) to successfully control the frequency using the equation as a signal for monitoring [31]. The frequency shift that occurs during disturbance occurrences and the power transfer between one or more locations are the variables that make up the ACE equation. If load or power variations induce frequency or power deviations on the tie-line, the AGC will quickly restore stability. Because RES uncertainty is a constant source of power imbalance in the power system, this AGC system is vital nowadays. When the system's generating power and load balance changes, AGC uses ACE to set it to zero. System frequency variations and exchange power between the two regions are components of the ACE signal. When a power outage happens in one portion of the power grid, the algorithm will try to fix it as soon as possible in that same part of the grid. In such region, AGC secondary control modifies things so that power balance is restored. The following equations show the ACE and associated element expressions [32]:

$$ACE_i = \Delta P_{ij} + \beta_i \Delta f$$

$$\Delta P_{ij} = \sum_{k=1}^{K} Pflow_k - Pflow_{ref}$$

$$\Delta f = f_{meas} - f_{ref}$$

The variables ACE_i, ΔP_{ij}, γ_i, and Δf represent many variables in the power system, including the area control error of area i, 'the tie-line power flow error between bus i and j, the frequency bias coefficient of area i, and the frequency error." The second equation displays the deviation of the interchange power, where "P_{flowk} is the exchange power on tie-line k and K tie-lines link two locations in total." When talking about power flow in tie-lines, $Pflow_{ref}$ is the standard. In the third equation, we can see the system's frequency error, "where f_{ref} is the nominal frequency and f_{meas} is the measurement frequency at the rotor [32]."

In both locations, the AGC controller is used to get the "ACE_i values, which are ACE1 = ΔP12 + β1Δf and ACE2 = ΔP21 + β2Δf." The generators in Area 1 have sufficient spinning reserves to restore the frequency to its nominal value (ACE1 = 0), in the event that frequency deviation is caused by the reduction in the producing capacity of the power source in Area 1. Area 2's production and tie-line f low remain unchanged since the power adjustment at the generators is limited to Area 1. "Even if Area 1's reserve capacity is insufficient, ACE1 will continue to exist due to the non-zero value of Δf. Currently, in order to offset Area 1, the surplus power from Area 2 is sent to the remaining ΔP12 and Δf, bringing ACE1 down to 0. At fref, the frequency remains stable." Area 2's power output more than makes up for Area 1's power deficit. If the secondary control's reserve power is sufficient, this controller may essentially return the frequency to a steady fref value. When enough electricity is supplied from one location to support another, the frequency will be stabilized.

"Equation may be used to represent the proportional-integral (PI) of ACE_i over a certain time period in the Laplace domain [32]:"

$$P_{AGC}(s) = \left(K_p + \frac{K_i}{s}\right) \cdot ACE_i(s)$$

"The P_{AGC} signal, after passing through the PI controller, will be multiplied by each participation coefficient of the generators in the AGC system λ^g_i, finally obtaining the dp^g_i signal sent to the governor of the generator *g* in area *I [32]*:"

$$dp_i^g = P_{AGC} \cdot \lambda_i^g$$

$$\lambda_i^g - \frac{P_{\max_i}^g}{\sum_g P_{\max_i}^g}$$

The typical way of finding the AGC system generators' participation coefficients, denoted as $\lambda^g{}_i$, is given by the equation above. Typically, "it is selected based on the ratio of the overall maximum power of the generators involved in the secondary frequency modulation ($\sum$ g $P^g max_i$) to the maximum power of the generator g ($P^g max_i$)." On the other hand, when power imbalance events happen repeatedly in the system, this strategy won't guarantee the quantity of frequency control capacity. Hence, in order to decrease the generators' transients, the selected $\lambda^g{}_i$ coefficients should be more than the value computed using the previous Equation but less than 1. Figure 1 depicts the AGC system's transfer function, whereas Figure 2 shows the composite model.

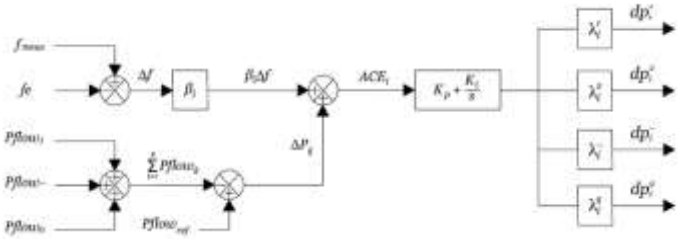

Figure 1: The transfer function of the AGC system.

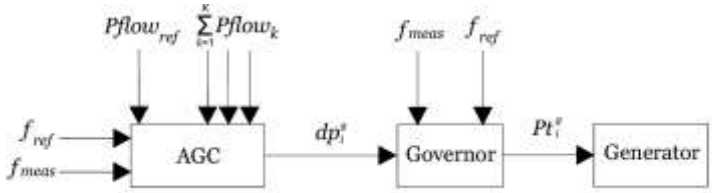

Figure 2: The composite model of the AGC system.

B. I-TD Controller

A novel secondary controller, denoted by TID, was created by Lurie et al. [15]. It combines the best features of controllers with integer and fractional orders. The structure of TID is similar to that of PID, with the exception that 1/s^(1/N) is multiplied by the proportional term of PID. The following equations provide the transfer functions of PID and TID.

$$G_{PID}(s) = K_{P,PIDi} + \frac{K_{I,PID\,i}}{s} + K_{D,PIDi}s$$

here "$K_{P,PIDi}$ is proportional gain , $K_{I,PIDi}$ is integral gain and $K_{D,PIDi}$ is derivative gain of PID controller."

$$G_{TID}(s) = \frac{K_{T,TIDi}}{s^{(1/N_{TIDi})}} + \frac{K_{I,TID\,i}}{s} + K_{D,TID_i}s$$

where "$K_{T,TIDi}$ is tilt gain , $K_{I,TIDi}$ is integral gain , $K_{D,TIDi}$ is derivative gain and $N_{,TIDi}$ is real number ($N_{,TIDi} \neq 0$) of TID controller."

One undesirable side effect of using derivative control in forward paths is the generation of derivative kick, which may disrupt electronic circuits. Industrial engineers have rethought TID's structure as I-TD, with the tilt and derivative terms in the forward route and the integral terms in the feedback path, to circumvent this issue [15]. There has been no research on this I-TD controller for three-area multi-source AGC studies as of yet. Figure 3 shows the I-TD controller's construction, and the equations below describe its transfer function.

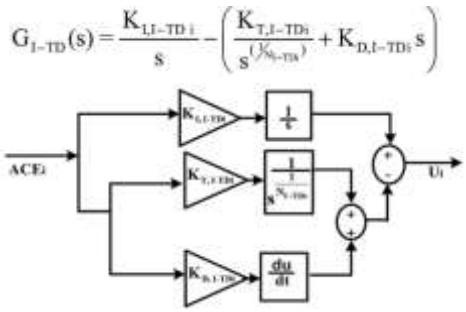

"Figure 3: Transfer function model of I-TD controller

where, KT,I-TDi is tilt gain, KI,I-TDi is integral gain, KD,ITDi is derivative gain and N,I-TDi is real number (N,TIDi ≠ 0) of I-TD controller." By applying a set of restrictions in the following equation and minimizing the objective function, the FA, GWO, and GHA techniques maximize the I-TD controller gains and other parameters all at once.

$$\left.\begin{aligned} 0 \le K_{P,PIDi} / K_{T,TIDi} / K_{T,I\text{-}TDi} \le 1 \\ 0 \le K_{I,PIDi} / K_{I,TIDi} / K_{I,I\text{-}TDi} \le 1 \\ 0 \le K_{D,PIDi} / K_{D,TIDi} / K_{D,I\text{-}TDi} \le 1 \\ 2 \le N_{TIDi} / N_{I\text{-}TDi} \le 7 \end{aligned}\right\}$$

2. Related works

In [33], the authors compared the performance of "PID with a double derivative controller to that of I/PI/PID controllers in an AGC system." Also, in realistically restricted situations like "GRC, GDZ, TD, and BD, conventional controllers may not always provide the best transient response. In the face of a wide range of step load magnitudes, the fundamental methods used by traditional controllers fail to provide satisfactory dynamic output." In addition, "AGC using FLC and Artificial Neural Networks (ANNs) has been the subject of several studies [40]." When compared to conventional controllers, the FLC-based AGC system's outputs are better optimized by adjusting the following parameters: "rule base, membership feature selection, scaling factor, and defuzzification technique." Nevertheless, analyzing and training the database using FLC and ANN takes a lot of computing effort.

To address the problem of load frequency regulation in a multi-area linked multi-source power system, Ahmed et al. (2021) [34] created an "integral derivative-tilted (ID-T) controller, which is a modified version of the tilted integral derivative (TID) controller." In addition, the suggested ID-T controller settings were fine-tuned using a novel optimization approach called the Archimedes optimization algorithm (AOA). A two-area linked power system was used to assess the performance of the proposed ID-T controller based on AOA. "Each area had a variety of conventional generating units, including thermal, gas, and hydraulic power plants, as well as renewable power sources, such as wind and solar power. In addition, the suggested controller took system uncertainties, generation rate limits, governor deadband, and communication time delays into account, as well as swings in demand and renewables." As shown in the simulation results, the proposed ID-T controller based on the AOA significantly improved the frequency stability of the system under various scenarios involving various load perturbations, uncertainties in the system, physical constraints, communication time delays, and high penetration of renewable energy sources.

Electric vehicles (EVs) and high-voltage direct current (HVDC) links were investigated in a study by Chiranjeevi et al. (2025) [24]. An HVDC-linked thermal unit was part of the proposed system that EVs were a part of. As an auxiliary controller, a new controller called the integral minus tilt double derivative

(I-TD2N) has been designed. By using the Mayfly optimization algorithm (MOA), the controller parameters were successfully adjusted. After evaluating the system's dynamic responses with three different controllers, “PID, TID, and I-TD2N”, it was determined that the latter provided the most effective performance. Additionally, the best performance index was determined by comparing ISE, ITSE, IAE, and ITAE. Research indicates that ISE converges more quickly than competing methods. Research using an HVDC link shown that these connections improve the dynamic performance of the system. The integration of the HVDC connection with the EVs also greatly enhanced the dynamic reactions. To further assess the recommended I-TD2N controller's robustness under different loading conditions, a sensitivity analysis was also conducted.

For the Maglev system, Sain et al. (2016) [35] suggested an I-TD controller architecture and compared its performance to that of a traditional TID controller. This research used a genetic algorithm (GA) to optimize the TID controller settings, and the resulting set of values was used to create an I-TD controller. After that, we looked at how well the TID controller and the I-TD controller performed. Results for maximum overshoot, gain margin, and phase margin demonstrate that the I-TD controller is better than the TID controller. Both examples had about the same settling time.

The request for an integral minus tilt derivative controller (I-TD) in a three-area AGC system that incorporated renewable energy sources (RES) was studied by Babu et al. (2025) [36]. Methods based on the Mayfly optimization algorithm (MOA) were used to improve the system and controller settings. The proposed I-TD controller demonstrated its efficacy by outperforming traditional TID and PID controllers in terms of settling time (ST), overshoots (OS) (by 53%), and undershoots (US) (by 50%). Additionally, the benefits of integrating HVDC and RES lines into the system's dynamics were investigated. By integrating RES by 23% and HVDC linkages by 45%, it was shown that dynamics in terms of OS, US, and ST much improve.

When it comes to improving the load frequency management mechanism of interconnected power systems, Raj and Shankar (2023) [37] addressed the intermittent nature of renewable energy sources and electric cars. A secondary focus of this study was the effect of communication delay on the long-term viability of the system. A thermal plant, hydro plant, and gas plant were all components of the two-area linked hybrid power system that was the subject of the mathematical modeling and analysis that was conducted. In addition, for the sake of the case study, both control zones additionally included electric cars and intermittent solar and wind power facilities. The examined system contains a unique tilt controller that is a cascade of fractional-order integral-derivatives. To further optimize the various controller settings, a modified Quasi-Opposition Reptile Search Algorithm (QORSA) is also suggested. A number of well-known meta-heuristic algorithms over the last several years were compared to the QORSA in order to prove its superiority.

3. Present Work and Methods

A "two-area interconnected power system" is one in which the two control areas are linked by a tie line. The tie line allows electricity to travel across sections in this system, while each area supplies power to its own region. “The Two Area Interconnected Power System is a small system that incorporates models of the turbine, governor, synchronous generator (mass spinning), and load into each of its areas. Commonly used in mathematical modeling of this system for control system analysis and design, the transfer function (Fig. 4) is one of the most prominent approaches.” First, using the swing equation based on a thin incremental change, one may construct the model of the generating unit. After that, we'll

use Eq. [27] as is for the Laplace transform:

$$\Delta\Omega(s) = \frac{1}{2Hs}(\Delta P_m - \Delta P_e)$$

"where the variables Ω(s) for generation speed, H for generation inertia, ΔPm for mechanical power variation, and ΔPe for electrical power fluctuation are represented." There are two kind of loads: "those that are independent of frequency (such as a resistive load) and those that are sensitive to frequency variation (such as motors)."

$$\Delta P_e = \Delta P_L + D\Delta\omega$$

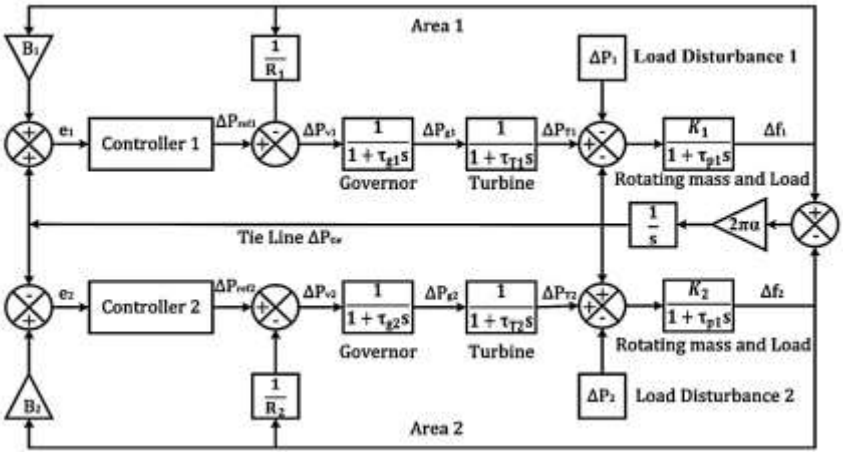

Figure 4: "The proposed two area interconnected AGC power system"

When the sensitive-load is denoted by D$\Delta\tau$ and the constant sensitive load is represented by PL. Lastly, the generator (the mass that rotates) and the load are represented by a gain K and a time constant BP, respectively, as shown below:

$$\frac{\Delta\Omega}{\Delta P_m(s) - \Delta P_e(s)} = \frac{K}{1+\tau_P s}$$

Modifying the location of the steam valve causes the turbine to generate mechanical power in a proportionate manner, as shown by

$$\frac{\Delta P_m(s)}{\Delta P_v(s)} = \frac{1}{1+\tau_T s}$$

In this case, τT stands for the standard speed turbine time constant. "A speed governor's primary function in a turbine is to change the output power Pg by adjusting the system's power ΔΩ/R and the reference power Pref."

$$\Delta P_g = \Delta P_{ref} - \frac{\Delta\Omega(s)}{R}$$

where the variable speed regulator is represented by R. As the connected load increases, the turbine's rotational speed decreases. "We may assume that it follows a straight line from the specified transfer function to the time constant Bg."

$$\frac{\Delta P_v}{\Delta P_g} = \frac{1}{1+\tau_g}$$

The three inputs identified in Fig. 5, which represent a single control region, are the following: l"oad disturbance ΔP, tie line power ΔPtie, and the power reference ΔPref." The output of these systems is

represented by "the area control area e error and the frequency error Δf. Here is the formula for the area control area e:"

$$e = -B\Delta f \mp \Delta P_{tie}$$

$$B = \frac{1}{R} + D$$

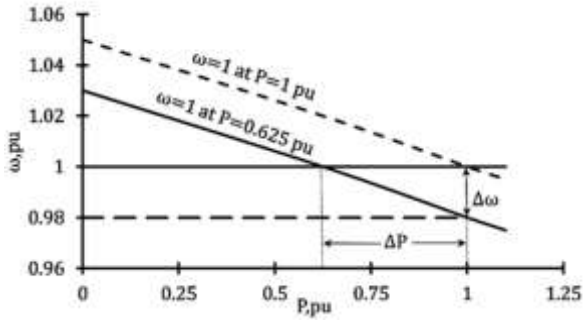

Figure 5: "Steady state speed characteristics of the governor"

In their proposal, Meng et al. [28] put forward the BSA. Based on the cooperative nature of bird swarms, it operates on the notion of swarm intelligence. Several things contribute to the birds' intelligence, such as their foraging skills, flying ability, and vigilant behavior. There are primarily three ways to navigate the BSA: (i) by hunting for food, (ii) by being vigilant when threatened, and (iii) by fleeing from the predator. According to [28], BSA's foraging behavior is described.

$$X_{p,q}^{i+1} = X_{p,}^{i} + (P_{p,q} - X_{p,q}^{m}) \times D \times rand_j(0,1) + (g_p - X_{p,q}^{i}) \times t \times rand_j(0,1)$$

in where p, i=1, 2,..., D-dimension, Pp,q denotes the previous position, gp is the swim position, and t denotes the step time. The vigilance and flight behaviors of BSA are also represented by Equations.

$$\left.\begin{aligned} X_{p,q}^{i+1} &= X_{p,q}^{i} + A_1\left(mean_q - X_{p,q}^{m}\right) \times rand_i(0,1) \\ &+ A_2\left(P_{p,q} - X_{p,q}^{m}\right) \times rand_i(-1,1) \end{aligned}\right\}$$

$$\left.\begin{aligned} X_{p,q}^{i+1} &= X_{p,q}^{n} + randn_i(0,1) \times X_{p,q}^{i} \\ X_{p,q}^{i+1} &= X_{p,q}^{i} + \left(X_{p,q}^{i} - X_{p,q}^{j}\right) \times fll \times rand_i(0,1) \end{aligned}\right\}$$

"where 0≤(A1, A2)≤2, randi (0/1), 0≤fll≤2. The Fig. 1(b) shows the flow chart of BSA and Fig 1(a) shows the optimised proposed BSEI-TD Controller."

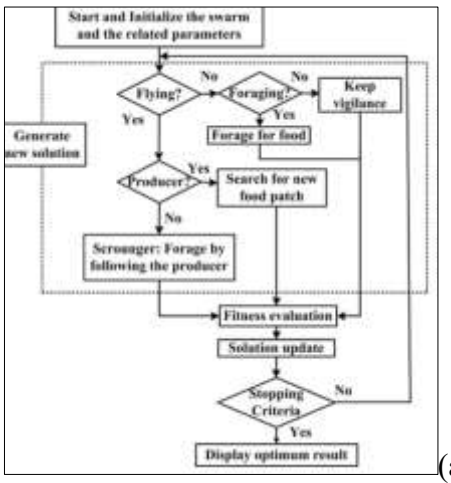

(a)

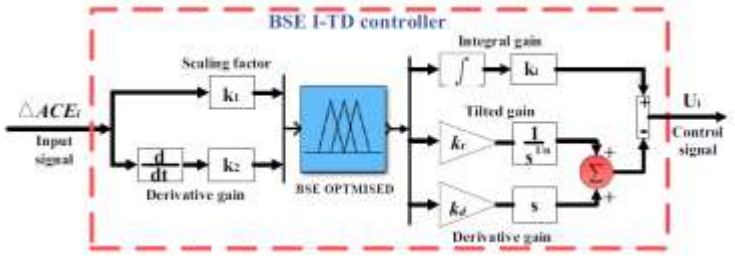

(b)

Figure 6: The Optimised BSEI-TD controller structure.

Input: Mutant, mixrate, N and D
Output: T, Trial Population

map(1:N, 1:D) = 1 // Initial map is an N-by-D matrix of ones

0. if a < b ~ U(0,1) then
1. for i from 1 to N do
2. map(i, u(Tmin:interrand:D)) = 0 | u = permuting (1, 2, 3, ..., D)
3. end
4. else
5. for i from 1 to N do, map(i, rand(D)) = 0, end
6. end
7. T := Mutant // Initial T
8. for i from 1 to N do
9. for j from 1 to D do
10. if map(i, j) = 1 then T(i, j) := P(i, j)
11. end
12. end

Algorithm 1. Crossover Strategy of BSA

Input: T, search space limits (i.e., low_j, up_j)
Output: T

for i from 1 to N do
for j from 1 to D do
if (T_{i,j} < low_j) or (T_{i,j} > up_j) then
T_{i,j} = rand·(up_j − low_j) + low_j
end
end
end

Algorithm 2. Boundary condition mechanism of BSA

4. Results and Discussion

Both the traditional I-TD and the suggested BSEI-TD controllers have their tuned parameters shown in Table 1. The BSEI-TD controller has a proportional gain of 0.0260, which indicates more control flexibility, compared to the I-TD structure, which does not have the proportional gain. An improvement in the balance between steady-state precision and transient responsiveness is seen in the proposed BSEI-TD's somewhat lower value of 0.2997 for integral gain compared to the I-TD controller's 0.3215. Better dynamic control and improved damping capabilities are shown by the slightly greater double derivative gain of BSEI-TD compared to I-TD.

Table 1: ***Tuned I-TD/BSEI-TD controller parameters***

Controller parameters	I-TD	BSEI-TD
Proportional gain (KP)	–	0.0260
Integral gain (KI)	0.3215	0.2997
Double derivative gain (KDD)	0.1704	0.1819

The two-area automated generation control system's settling time and ITAE performance were compared in Table 2. Both the settling time and the error index are greatest for the conventional BFOA based PID,

suggesting that it responds slowly and rejects disturbances poorly. Notable improvements have been made by the firefly optimized PID and hybrid firefly pattern search PID. However, when compared to advanced structures, their dynamic regulation is still restricted. Traditional PID and TID controllers further exhibit the benefit of modified derivative and tilt operations by reducing frequency deviation and tie line power oscillations. By moving the integral action to the feedback route, the I-TD controller is able to achieve reduced ITAE and quicker settling. A considerable decrease in the value of ITAE and the minimal settling time in both area frequencies are recorded by the suggested BSEI-TD controller. We can affirm that our load correction capacity is accurate and that our transient stability is greater. The BSEI-TD method guarantees a quicker recovery to nominal operating conditions and increases the AGC system's resilience during step load disruption, as shown by the comparison findings.

Table 2: "Comparative performance of error and settling time for two area power system"

Techniques/Controller	ΔF_1 T_s (s)	ΔF_2 T_s (s)	ΔPTie T_s (s)	ITAE
BFOA:PID [39]	14.2	13.0	14.2	2.3972
FA:PID [40]	10.0	10.1	9.9	1.3668
hFA-PS:PID [40]	7.9	6.8	7.2	1.078
PID	6.7	5.2	6.8	0.8977
TID	5.8	4.1	6.4	0.8595
I-TD	6.2	3.8	5.4	0.7600
Proposed BSEI-TD	5.7	2.8	6.4	0.6202

Figure 4 illustrates the dynamic responses of frequency and tie line power deviation for a two area system under a one percent step load disturbance in area one. The response in part (a) shows that the proposed BSEI-TD controller achieves faster damping of frequency oscillations in area one compared with BFOA-PID, FA-PID, hFA-PS-PID and conventional I-TD controllers. In part (b), the frequency deviation of area two follows a similar pattern where the proposed controller reaches steady condition in a shorter time with lower peak magnitude. Part (c) presents the tie line power deviation, indicating that the BSEI-TD approach effectively minimizes power exchange oscillations between the areas. The comparative curves confirm improved transient stability, reduced settling time and better suppression of overshoot through the optimized controller action.

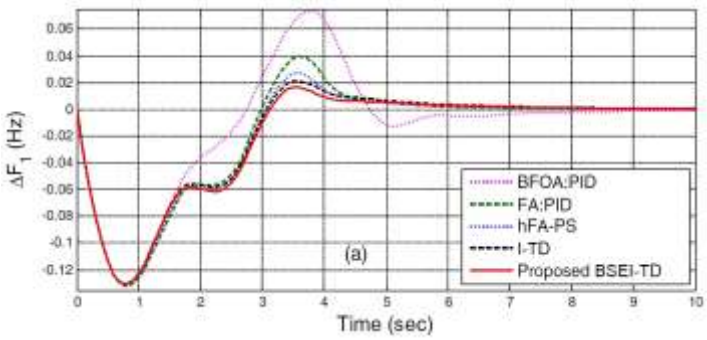

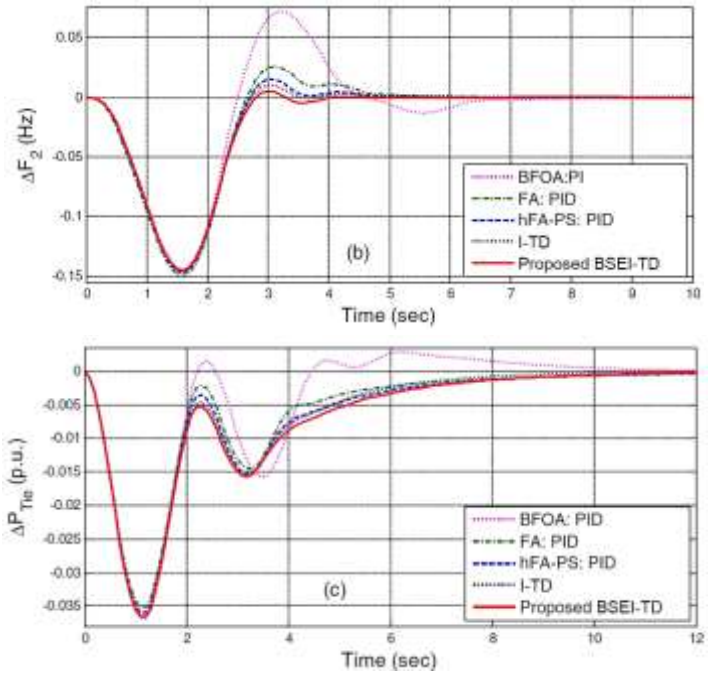

Figure 4: "Dynamic responses of two-area multi-source power system for 1% step load increase in area-1. (a) Frequency deviation of area-1. (b) Frequency deviation of area-2. (c) Tie-line power deviation."

Table 3: "Optimum gains and parameter of BSEI-TD controller at various loadings"

Loading Condition	Area	$K_{T,I\text{-}TD}$	$K_{I,I\text{-}TD}$	$K_{D,I\text{-}TD}$	$N_{I\text{-}TD}$
30% Loading	Area-1	0.4125	0.1484	0.9936	2.1475
30% Loading	Area-2	0.9760	0.1374	0.9979	5.4764
70% Loading	Area-1	0.8915	0.2424	0.3698	2.6291
70% Loading	Area-2	0.9992	0.0954	0.8942	3.8405

Optimal gains and settings of the BSEI-TD controller for two area systems under various loading situations are shown in Table 3. Area two has larger adaptation factor values and a steeper tilt, suggesting more robust corrective action, at thirty percent loading, in contrast to Area one's modest tilt and integral gains (with a derivative gain near to unity). Area one shows enhanced integral gain and decreased derivative component with 70% loading, whereas Area two requires various parameter choices to maintain frequency management. Confirming that the controller tuning adjusts well to different operating situations, area two with increased loading shows an increase in tilt gain with balanced derivative effects.

Figure 5 demonstrates the dynamic response of the two area system under different loading scenarios in comparison with the nominal fifty percent operating condition. Parts (a) and (b) present the frequency deviations of area one at thirty percent and seventy percent loading respectively. The curves show that the controller tuned for each specific loading condition provides quicker damping and smaller oscillatory magnitude than the parameters corresponding to nominal loading. Parts (c) and (d) illustrate the tie power deviation between the two areas for the same operating cases. The response with optimally tuned values for thirty percent and seventy percent loading exhibits faster convergence to zero with reduced peak variation. The results confirm that parameter adaptation according to operating point improves

transient stability and control accuracy. The comparison indicates that the BSEI-TD controller maintains effective regulation even when system loading changes significantly from the nominal condition.

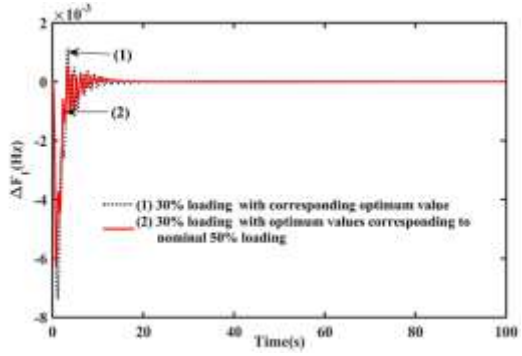

(a)

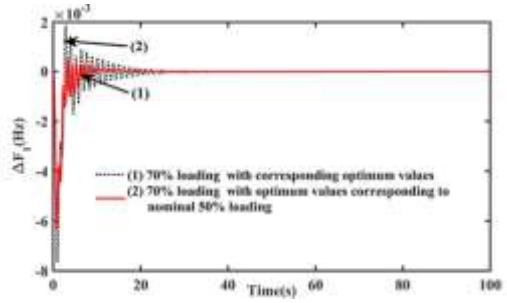

(b)

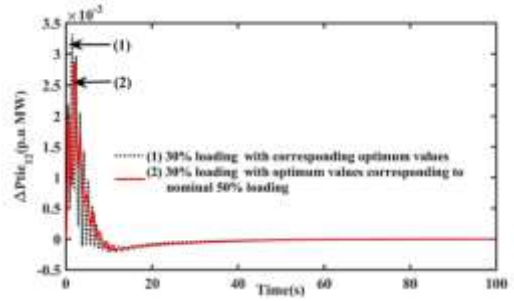

(c)

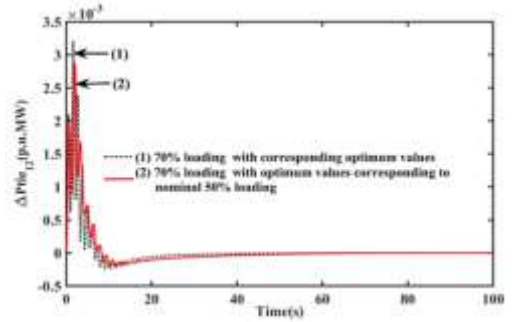

(d)

Figure 5: "Dynamic response comparison of the system at varied with nominal condition vs. time (a) Frequency deviation in area-1 at 30% loading condition, (b) Frequency deviation in area-1 at 70% loading condition, (c) Tie-power deviation among area-1 and area-2 at 30% loading condition and (d) Tie-power deviation among area-1 and area-2 at 70% loading condition."

5. Conclusion

The present work investigated the design of a Bird Swarm Algorithm based I-TD controller for a two area automatic generation control system. A comprehensive dynamic model of the interconnected power system was developed and the secondary controller parameters were optimised using the bio inspired BSA technique. Comparative analysis with PID, TID and other metaheuristic tuned controllers demonstrated the superiority of the proposed approach in terms of settling time, tie line power regulation and ITAE index. The optimised controller effectively reduced frequency oscillations in both areas and maintained scheduled power interchange under step load disturbances. Performance evaluation at thirty percent and seventy percent loading conditions verified the adaptability of the controller to different operating points. The results confirmed that appropriate tuning of tilt, integral and derivative components through BSA strengthens transient stability and enhances robustness of the AGC mechanism. The study establishes that the proposed BSEI-TD structure is a reliable solution for modern interconnected power systems with varying demand profiles.

6. References

1. O.I. Elgerd, C.E. Fosha, Optimum megawatt-frequency control of multiarea electric energy systems. IEEE Trans. Power App. Syst., 1970, pp. 556–563, vol. PAS-89no.
2. P. Kundur, “Power System Stability and Control,” Tata McGraw Hill, New Delhi, 5th edition, 1993
3. Sahu, R. K., Gorripotu, T. S., & Panda, S. (2015). Automatic generation control of multi-area power systems with diverse energy sources using Teaching Learning Based Optimization algorithm. *Engineering Science and Technology an International Journal*, *19*(1), 113–134. https://doi.org/10.1016/j.jestch.2015.07.011
4. Parmar, K. S., Majhi, S., & Kothari, D. (2012). Load frequency control of a realistic power system with multi-source power generation. *International Journal of Electrical Power & Energy Systems*, *42*(1), 426–433. https://doi.org/10.1016/j.ijepes.2012.04.040
5. Bhatt, P., Ghoshal, S., & Roy, R. (2010). Load frequency stabilization by coordinated control of Thyristor Controlled Phase Shifters and superconducting magnetic energy storage for three types of interconnected two-area power systems. *International Journal of Electrical Power & Energy Systems*, *32*(10), 1111–1124. https://doi.org/10.1016/j.ijepes.2010.06.009
6. Daneshfar, F., & Bevrani, H. (2012). Multiobjective design of load frequency control using genetic algorithms. *International Journal of Electrical Power & Energy Systems*, *42*(1), 257–263. https://doi.org/10.1016/j.ijepes.2012.04.024
7. Gozde, H., Taplamacioglu, M. C., & Kocaarslan, İ. (2012). Comparative performance analysis of Artificial Bee Colony algorithm in automatic generation control for interconnected reheat thermal power system. *International Journal of Electrical Power & Energy Systems*, *42*(1), 167–178. https://doi.org/10.1016/j.ijepes.2012.03.039
8. Ali, E., & Abd-Elazim, S. (2013). BFOA based design of PID controller for two area Load Frequency Control with nonlinearities. *International Journal of Electrical Power & Energy Systems*, *51*, 224–231. https://doi.org/10.1016/j.ijepes.2013.02.030
9. Ibraheem, Hasan, N., & Singh, O. (2011, April 6). *GASA tuned optimal fuzzy regulator for AGC of an interconnected power system*. https://www.ijcaonline.org/archives/volume20/number8/2451-2633/

10. Ranjitha, K., Sivakumar, P., & Rajapandiyan, A. (2022). Atom Search Optimization based Load Frequency Control and Firefly Algorithm based cost optimization for an interconnected power system with Renewable Energy Sources.
11. Saikia, L. C., Mishra, S., Sinha, N., & Nanda, J. (2011). Automatic generation control of a multi area hydrothermal system using reinforced learning neural network controller. *International Journal of Electrical Power & Energy Systems*, *33*(4), 1101–1108. https://doi.org/10.1016/j.ijepes.2011.01.029
12. Sharma, A., Parmar, K. S., & Gupta, S. K. Automatic Generation Control of Multi Area Power System using ANN Controller. *Transfer*, *120*(20s), 1.
13. Saha, A., and Saikia, L.C. (2017). Utilisation of ultra-capacitor in load frequency control under restructured STPP-thermal power systems using WOA optimised PIDN-FOPD controller. IET Distribution, Generation, Transmission and 11(13):3318-3331. https://doi.org/10.1049/iet-gtd.2017.0083
14. Sharma, Y., and Saikia, L.C. (2015). Automatic generation control of a multi-area ST-thermal power system using Grey Wolf Optimizer algorithm based classical controllers. *International Journal of Electrical Power and Energy Systems*, 73:853-862. https://doi.org/10.1016/j.ijepes.2015.06.005
15. Tasnin, W., and Saikia, L.C. (2018). Maiden application of a sine-cosine algorithm optimised FO cascade controller in automatic generation control of multi-area thermal system incorporating dish-Stirling solar and geothermal power plants. *IET Renewable Power Generation*, 12(5):585-597. https://doi.org/10.1049/iet-rpg.2017.0063
16. Babu, N.R., Sunitha, P., BSS, G.P., Bhagat, S.K., Ramesh, A., Saha, A., Mbasso, W.F., Jangir, P., and Hossam-Eldin, A. (2025). Enhanced automatic generation control in multiarea power systems: Crow search optimized cascade FOPI–TIDDN controller with integrated renewable solar thermal models and HVDC lines. *Engineering Reports*, 7(5):e70185. https://doi.org/10.1002/eng2.70185
17. Pan, I., and Das, S. (2015). Fractional order AGC for distributed energy resources using robust optimization. *IEEE Transactions on Smart Grid*, 7(5):2175-2186. https://doi.org/10.1109/TSG.2015.2459766
18. Babu, N.R., Saikia, L.C., and Raju, D.K. (2020). Maiden application of hybrid crow search algorithm with pattern search algorithm in LFC studies of a multi-area system using cascade FOPI-PDN controller. In Soft Computing for Problem Solving 2019: Proceedings of SocProS 2019 (Vol. 1, pp. 337 -351). *Springer Singapore*.
19. Golpira, H., and Bevrani, H. (2011). Application of GA optimization for automatic generation control design in an interconnected power system. *Energy Conversion and Management*, 52(5):2247-2255. https://doi.org/10.1016/j.enconman.2011.01.010
20. Saikia, L.C., Sinha, N., and Saha, D. (2017, April). Application of antlion optimizer technique in restructured automatic generation control of two-area hydro-thermal system considering governor dead band. In 2017 Innovations in Power and Advanced Computing Technologies (i-PACT) (pp. 1-6). IEEE. https://doi.org/10.1109/IPACT.2017.8245099
21. Dash, P., Saikia, L.C., and Sinha, N. (2015). Comparison of performances of several FACTS devices using Cuckoo search algorithm optimized 2DOF controllers in multi area AGC. International Journal of Electrical Power and Energy Systems, 65:316-324. https://doi.org/10.1016/j.ijepes.2014.10.015
22. Saikia, L.C., Chowdhury, A., Shakya, N., Shukla, S., and Soni, P.K. (2013). AGC of a multi-area gas-thermal system using firefly optimized IDF controller. In 2013 Annual IEEE India Conference (INDICON) (pp. 1-6). IEEE. https://doi.org/10.1109/INDCON.2013.6725998

23. Babu, N.R., Chiranjeevi, T., and Saha, A. (2024). Application of RT-Lab in multi-area AGC system under deregulated environment considering IPFC-SMES. Iranian Journal of Science and Technology, Transactions of Electrical Engineering, 48(4):1643-1656. https://doi.org/10.1007/s40998-024-00740-y
24. Chiranjeevi, T., Pardhu, B.G., Babu, N.R., Das, S., AboRas, K.M., Mbasso, W.F., Sunitha, P., Ramesh, A., Jangir, P., and Khishe, M. (2025). Impact of HVDC link and electric vehicle on multi-area power system using MOA optimized I-TD2N controller. Results in Engineering, 25:103901. https://doi.org/10.1016/j.rineng.2024.103901
25. Saha, A., Dash, P., Chiranjeevi, T., and Ram Babu, N. (2024). Implementation of combined hydrogen aqua electrolyser fuel cell and redox-flow battery under restructured situation of AGC employing TSA optimized PDN(FOPI) controller. Journal of Taibah University for Science, 18(1):2334004. https://doi.org/10.1080/16583655.2024.2334004
26. Li, J., and Zhou, T. (2025). A robust large-scale multiagent deep reinforcement learning method for coordinated automatic generation control of integrated energy systems in a performance-based frequency regulation market. IEEE/CAA Journal of Automatica Sinica, 12(7):1475 1488. https://doi.org/10.1109/JAS.2024.124482
27. Awal, M., Atim, M.R., Nabende, W.J., Obungoloch, J., and Barakat, M. (2025). Fire hawk optimizer adjusted tri-stage (1 + PI)-PITID cascade controller for automatic generation control of PSI. IEEE Access. https://doi.org/10.1109/ACCESS.2025.3577622
28. Meng, X., Gao, X., Lu, L., Liu, Y., & Zhang, H. (2015). A new bio-inspired optimisation algorithm: Bird Swarm Algorithm. *Journal of Experimental & Theoretical Artificial Intelligence*, *28*(4), 673–687. https://doi.org/10.1080/0952813x.2015.1042530
29. Bhagat, S.K., Saikia, L.C., and Babu, N.R. (2021). Effect of partial loading on a three-area hydro-thermal system integrated with realistic dish-Stirling solar thermal system, accurate model of high-voltage direct link considering virtual inertia and energy storage systems. International Transactions on Electrical Energy Systems, 31(12):e13169. https://doi.org/10.1002/2050-7038.13169
30. Bhagat, S.K., Saikia, L.C., and Babu, N.R. (2024). Inertia emulation control strategy of an accurate model of HVDC link in a multi-area automatic generation control system integrated precise wind turbine system. Iranian Journal of Science and Technology, Transactions of Electrical Engineering, 48(1):143-163. https://doi.org/10.1007/s40998-023-00641-6
31. Kundur, P.S.; Malik, O.P. Power System Stability and Control; *McGraw-Hill Education*: New York, NY, USA, 2022.
32. Lam, L.H.; Nam, L.K.; Dung, N.K.T.; Hieu, N.H. Two-Area Automatic Generation Control for Power Systems with Highly Penetrating Renewable Energy Sources. *Electronics* 2024, 13, 2907. https://doi.org/10.3390/electronics13152907
33. Raju, M., Saikia, L. C., & Sinha, N. (2016). Automatic generation control of a multi-area system using ant lion optimizer algorithm based PID plus second order derivative controller. *International Journal of Electrical Power & Energy Systems*, *80*, 52–63. https://doi.org/10.1016/j.ijepes.2016.01.037
34. Fathy, A., & Kassem, A. M. (2018). Antlion optimizer-ANFIS load frequency control for multi-interconnected plants comprising photovoltaic and wind turbine. *ISA Transactions*, *87*, 282–296. https://doi.org/10.1016/j.isatra.2018.11.035

35. Ahmed, M., Magdy, G., Khamies, M., & Kamel, S. (2021). Modified TID controller for load frequency control of a two-area interconnected diverse-unit power system. *International Journal of Electrical Power & Energy Systems*, *135*, 107528. https://doi.org/10.1016/j.ijepes.2021.107528
36. Sain, D., Swain, S. K., & Mishra, S. K. (2016). TID and I-TD controller design for magnetic levitation system using genetic algorithm. *Perspectives in Science*, *8*, 370–373. https://doi.org/10.1016/j.pisc.2016.04.078
37. Babu, N. R., Satyanarayana, S., Sai, A. B., Reddy, M. V. V. S. S., Reddy, T. V. S., Pooja, Kumar, M., & Chiranjeevi, T. (2025). Application of HVDC link in a RES integrated multi-area power system using MOA optimized I-TD Controller. In *Lecture notes in electrical engineering* (pp. 151–161). https://doi.org/10.1007/978-981-96-0058-8_12
38. Raj, U., & Shankar, R. (2023). Optimally enhanced fractional-order cascaded integral derivative tilt controller for improved load frequency control incorporating renewable energy sources and electric vehicle. *Soft Computing*, *27*(20), 15247–15267. https://doi.org/10.1007/s00500-023-07933-3
39. E.S. Ali, S.M. Abd Elazim, *BFOA based design PID controller for two-area Load Frequency Control with nonlinearities*, Int. J. Electr. Power Energy Syst. **51** (2013) 224–231.
40. R.K. Sahu, S. Panda, S. Padhan, *A hybrid firefly algorithm and pattern search technique for automatic generation control of multi-area power systems*, Int. J. Electr. Power Energy Syst. **64** (2015) 9–23.